NONLINEAR HETEROASSOCIATIVE SPECTRAL MEMORIES: VIRTUALLY PARTITIONED NEURAL ENCODERS AND DECODERS FOR DIGITAL COMMUNICATIONS

RONALD G. SPENCER
Analog & Mixed-Signal Center
Electrical Engineering Dept.
Texas A&M University
College Station, TX. 77843-3128
ron.spencer@ieee.org

ABSTRACT

Nonlinear heteroassociative spectral memories are introduced that extend previously introduced spectral associative memories (SAMs) to include networks with virtual neural layers. SAMs are quantized frequency domain formulations of recurrent associative memories in which data bits are encoded as phase of oscilation in attractor waves and recalled by recurrent spectral convolution. Due to *decoder/attractor separability*, *virtual non-local connectivity*, and *linear scalability*, SAMs are well suited for digital communications. Bit vectors may be transmitted over a noisy channel as a superposition of waves and recovered by spectral neural decoding. Due to the inherent redundancy of the encoding process, noise immunity is *built-in* and non-local connectivity is realized *virtually*, maintaining high symbol-to-bit ratios while scaling *linearly* with the input vector. Autoassociative SAMs achieve the highest noise immunity for a given *N*-dimensional bit pattern due to their full, virtual interconnectedness and high encoding redundancy, but do not allow for various *degrees* of such redundancy. Heteroassociative SAMs offer a compromise between encoding redundancy and bandwidth as they partition *N*-dimensional bit patterns into *virtual spectral layers*. Bit error rate simulations are presented for various degrees of convergence time, spectrum spread, and SNR.

INTRODUCTION

Hopfield introduced the recurrent autoassociative memory nearly two decades ago (Hopfield, 1982), in which bipolar patterns are stored in the synaptic weight matrix of a neural decoder and recalled by non-linear, recurrent feedback in the presence of noise. Several years later, Kosko introduced the heteroassociative associative memory (Kosko, 1987, 1988) in which bipolar pattern *pairs* are encoded and recalled in the same manner. These networks are categorized as *content addressable memories* (CAMs) because memory recall is initiated by partial or noisy patterns and carried out without an address.

Associative memories bear a strong resemblance to holograms (Gabor, 1969), (Psaltis, 1985, 1990), (Owechko, 1989), due to the redundancy of stored patterns in the matrices that specify neural connectivity. In the Hopfield network, every neuron‘s local synaptic weight vector contains information about the *global* pattern. Like a hologram, the *parts make up the whole* and the *whole makes up the parts*; contained within the pieces of a broken hologram is the entire image itself. Such high degrees of redundancy lead to noise immunity, but usually at the expense of spatial dimension. Unlike cellular neural networks (Chua, et al., 1993), which are locally connected, CAMs are non-locally connected and therefore scale quadratically or polynomially.

Spectral associative memories (SAMs) (Spencer, 2000) are associative memories realized in the frequency domain, in which memory *waves* serve as network attractors. Exploiting the reversible property of the superposition of orthogonal waves and the richness of *spectral convolution*, non-local connectivity is achieved *virtually*, reducing network dimensions and allowing the attractor to be separated from the neural decoder. Whereas the attractors in conventional CAMs are *spatially embedded* in the network as an array of synaptic weights, spectral attractors persist as a superposition of waves that activate a neural decoder *transiently* (see Figure 1). Fortunately, attractor waves lend themselves to carrying digital information over a noisy channel, which may be recovered by a remote decoder. Until activated by one or more waves, the spectral neural decoder is an *uninstantiated, attractorless decoder* with no net motive; only when activated with *colored motive*, is one of the memories expanded (recalled). When limited to transmitting and receiving one encoded memory wave at a time, spectral encoders and decoders are well suited for robust digital telecommunications in the presence of noise.

Fortunately, spectral associative memories scale *linearly* with pattern dimension, while maintaining the same high encoding redundancy as spatial associative memories. Redundancy is manifested in the frequency domain rather than spatial connectivity; i.e. redundancy increases bandwidth, rather than network dimension. Autoassociative spectral memories achieve the highest noise immunity due to their full, virtual interconnectedness; however, bandwidth scales quadratically with codeword dimension. And for a given codeword length, the code rate is *forced* on the designer.

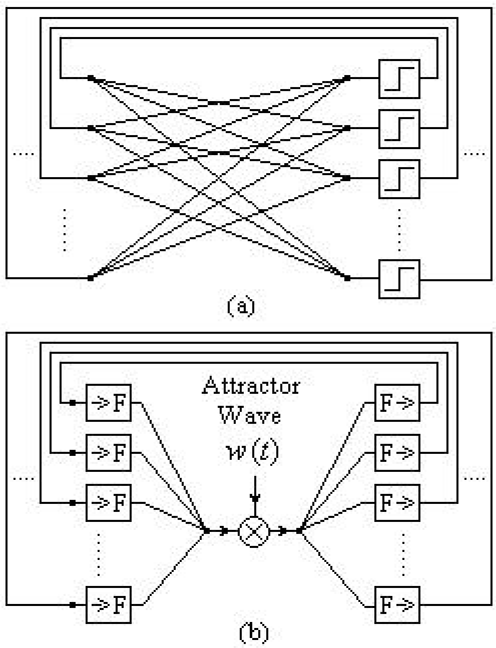

Fig. 1. Two realizations of the Hopfield decoder: (a) spatial and (b) spectral. Blocks labeled "->F"/"F->" mean "to/from frequency domain".

For the same number of neurons partitioned into two virtual layers, heteroassociative spectral memories allow for various degrees of encoding redundancy. In the heteroassociative spectral memory, the degree of *virtual* connectivity is less than that of the autoassociative spectral memory, reducing attractor wave bandwidth by a factor of N_1N_2/N^2 and the number of encoding oscillators by half. This additional degree of freedom offers a way to balance the tradeoff between encoding redundancy and noise immunity on one hand, and number of oscillators and memory wave bandwidth on the other.

Autoassociative spectral memories are briefly reviewed in the next section followed by heteroassociative spectral memories in the third section. Single attractor networks for digital communications are discussed in the fourth section along with bit error rate simulations in the presence of noise. Scaling complexity of potential implementations are discussed in the fifth section followed by conclusions in the sixth section.

AUTOASSOCIATIVE SPECTRAL MEMORIES

With quantized spectral processing, the Hopfield network may be reformulated in the frequency domain where memories are manifested as *attractor waves* which instantiate a spectral neural decoder, rather than a synaptic weight matrix (Spencer, 2000). As such, attractors may exist *separately* from the neural decoder as a superposition of waves. This allows non-local connectivity to be realized virtually, by spectral convolution. Recalled data bits are simultaneously represented in the spatial domain as quantized neural states and in the frequency domain as *quantized phase of oscillation*; i.e. the state of each local oscillator may change only by discrete amounts, or *phase quanta*. Like photons in an electromagnetic field, electrons in a matter field, phonons in a vibrating silicon lattice, or corticons in a biomolecular vibration field (Jibu and Yasue, 1993, 1995), such discrete changes may be regarded as something like an *associaton* in a vibrating association field. In the same way that electrons minimize the energy state of an atom by jumping from one eigenstate to another, releasing electromagnetic quanta (photons) along the way, local changes in phase occur during recall, driven by the tendency of the Hopfield formalism to reduce global network energy. Seemingly spontaneous local "jumps" in neural state lead to discrete reductions in global error, causing quantum *releases* in energy where the energy landscape is instantiated by the attractor waves that activate the network. With nonlinear processing, the decoder *chooses* one memory among several that exist in coherent linear superposition in the attractor wave.[1] Quantum computation itself may prove to be an efficient means of realizing associative memories (Ventura and Martinez, 1998), taking advantage of the linearity of Schrödinger's wave equation (Schrödinger, 1926) and the nonlinearity of measurement.

Autoassociative spectral decoding consists of three simultaneous processes: 1) spectral synthesis, 2) spectral convolution, and 3) spectral analysis,

$$v_i = \mathrm{sgn}\left(\int w(t) v(t) \cos(\omega_{Ai} t) dt \right) \tag{1}$$

$$v(t) = \sum_{i=0}^{N-1} v_i \cos(\omega_{Vi} t); \quad i = 0,1,\ldots N-1 \tag{2}$$

where v_i is the i^{th} recalled bit and neural state, $w(t)$ is the attractor wave which carries at least one spectral attractor, $v(t)$ is the continuously updated state wave, and ω_{Ai} and ω_{Vi} are the analysis and synthesis frequencies of the i^{th} recalled bit, respectively, which must be defined to avoid aliasing.

[1] However, the memory wave here does not collapse upon observation (decoding), due to the classical nature of computation.

The single-memory version of the attractor wave is defined as,

$$w(t) = \frac{2\sqrt{P_s}}{N}\left(\sum_{i=0}^{N-1} b_i \cos\left(\omega_{S1_i} t\right)\right)\left(\sum_{i=0}^{N-1} b_i \cos\left(\omega_{S2_i} t\right)\right) \quad (3)$$

where $b_i \in \{-1,+1\}$ is the i^{th} encoded bit, ω_{S1i} and ω_{S2i} are the 1st and 2nd encoding frequencies of the i^{th} encoded bit, and P_s is the desired signal power.

Autoassociative spectral memories achieve the highest noise immunity due to their full, virtual interconnectedness, but the price is paid in bandwidth. For N-bit patterns, the bandwidth of the lower side-band of the attractor wave is N^2, achieving a *symbol-to-bit ratio*, or *code rate*, of N:1. This is *fixed* for an N-bit codeword and autoassociative SAMs do not allow for various *degrees* of encoding redundancy.

HETEROASSOCIATIVE SPECTRAL MEMORIES

Bidirectional associative memory networks may also be reformulated in the frequency domain with quantized spectral processing, in which memories are manifested as attractor waves. Compared to autoassociative SAMs, these networks offer an added degree of flexibility in satisfying the tradeoff between encoding redundancy and bandwidth by codeword *partitioning*. Whereas autoassociative attractor waves consist of N^2 frequencies, heteroassociative attractor waves consist of N_1N_2 frequencies, where $N_1+N_2=N$. Thus, for a given N-bit codeword, a number of different code rates are possible. A 5-bit codeword, for example, may be partitioned into {1,4} or {2,3}, generating 4 or 6 cosine waves, respectively, versus 25 in the autoassociative case. Furthermore, the code rate of bits in the *shortest* virtual layer are always *higher* than those in the longest layer and thus have greater noise immunity. Thus, encoding redundancy may be tailored to data significance as most significant bits may be represented by neurons in the least populated layer.

Spectral Encoding

The composite attractor wave may be constructed by superposing p attractor waves, each representing one encoded pattern generated by spectral convolution from two encoder waves, $s_1^{(m)}(t)$ and $s_2^{(m)}(t)$, (see Figure 2a),

$$w(t) = \frac{2}{p}\sqrt{\frac{P_{\max}}{N_1 N_2}}\sum_{m=1}^{p} s_1^{(m)}(t)\, s_2^{(m)}(t) \quad (4)$$

where p is the number of pattern pairs and P_{max} is the maximum signal power, which occurs when all patterns constructively reinforce. The encoder waves are weighted superpositions of cosine waves,

$$s_1^{(m)}(t) = \sum_{i=0}^{N_1-1} b_{1,i}^{(m)} \cos\left(\omega_{S_{1,i}} t\right) \quad (5)$$

$$s_2^{(m)}(t) = \sum_{j=0}^{N_2-1} b_{2,j}^{(m)} \cos\left(\omega_{S_{2,j}} t\right) \quad (6)$$

where $b_{1,i}$ and $b_{2,j}$ are the 1st and 2nd layer bits {-1,+1}, respectively, of the two bipolar vectors to be encoded, and $\omega_{S1,i}$ and $\omega_{S2,j}$ are 1st and 2nd layer radial encoding frequencies, respectively. Encoding frequencies must be placed at regular intervals such that spectral autocorrelation is enforced,

$$\omega_{S_{1,i}} := \omega_{S1.L} + N_2(N_1 - 1)\Delta\omega - i\Delta\omega \quad (7)$$

$$\omega_{S_{2,j}} := \omega_{S2.L} + j\Delta\omega \quad (8)$$

where $\Delta\omega$ is the radial frequency separation and $\omega_{S1.L}$ and $\omega_{S2.L}$ are the lowest frequencies in the respective bands for i=0,1,…N_1-1 and j=0,1,…N_2-1.

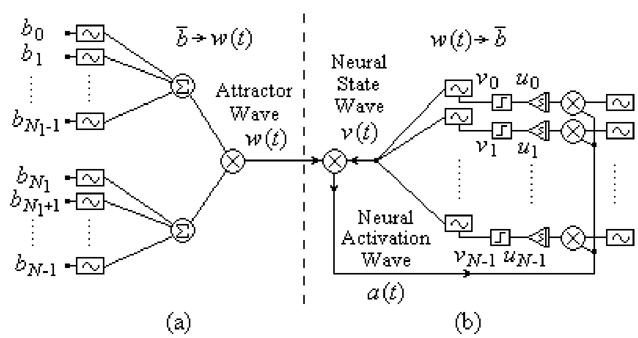

Fig. 2. Schematic of a single-memory, heteroassociative spectral encoder/decoder pair for N-bit codewords partitioned into N_1 and N-N_1 bits.

Each pattern in (4) generates a *spectral attractor* in the *lower side-band* of $w(t)$ of bandwidth $(N_1N_2\text{-}1)\Delta\omega$. Each bit in the 1st and 2nd virtual layers generate N_2 and N_1 frequencies in the attractor wave, thus the symbol-to-bit ratio of 1st layer bits is N_2:1 and the symbol-to-bit ratio of 2nd layer bits is N_1:1. The upper side-band contains no useful information for decoding and should be filtered out, but it is possible to recover the original patterns without doing so.

Spectral Recall

Spectral recall is *recurrent spectral processing* that consists of three simultaneous processes: 1) synthesis, 2) convolution, and 3) analysis. See Figure 2b. The attractor wave is spectrally convolved with the *state wave*, $v(t)$, to produce the *neural activation wave*, $a(t)$, in which linear activation information exists. Linear activation information is then directly modulated down to DC, integrated, and quantized to determine neural states. This continuous process decreases network energy over time and expands one of the patterns carried in the attractor wave.

Spectral Synthesis. Spectral synthesis is the construction of the state wave, $v(t)$, which represents the state of the system in the frequency domain. The state wave is defined as the sum of two virtual layer state waves,

$$v(t) = v_1(t) + v_2(t) \tag{9}$$

where $v_1(t)$ and $v_2(t)$ are the 1st and 2nd virtual layer state waves, which carry the state of the neurons they represent as quantized amplitudes, or equivalently, as quantized phases. Each virtual layer state wave is a linear superposition of N *evenly synchronized (cosine) waves*[2], with frequencies ascending from lowest to highest,

$$v_1(t) = \sum_{i=0}^{N_1-1} v_{1,i} \cos\left(\omega_{V_{1,i}} t\right); \qquad \omega_{V_{1,i}} := \omega_{V1.L} + N_2 i \Delta\omega \tag{10}$$

$$v_2(t) = \sum_{j=0}^{N_2-1} v_{2,j} \cos\left(\omega_{V_{2,j}} t\right); \qquad \omega_{V_{2,j}} := \omega_{V2.L} + j \Delta\omega \tag{11}$$

where $v_{1,i}$ and $v_{2,j}$ are 1st and 2nd layer recalled bipolar bits {-1,+1} and $\omega_{V1,i}$ and $\omega_{V2,i}$ are the 1st and 2nd layer *synthesis* frequencies.

Spectral Convolution. Non-local connectivity may be achieved *virtually* by spectrally convolving the state wave with the attractor wave,

$$[a(t) = w(t)v(t)] \leftrightarrow [A(\omega) = W(\omega) * V(\omega)] \tag{12}$$

which generates N_1+N_2 linear combinations in the lower side-band of $a(t)$.

Spectral Analysis. Activation information may be extracted from the activation wave by direct, local conversion followed by integration, and quantization,

$$v_{1,i} = \mathrm{sgn}(u_{1,i}); \quad u_{1,i} = c\int a(t)\cos\left(\omega_{A_{1,i}} t\right)dt \tag{13}$$

$$v_{2,j} = \mathrm{sgn}(u_{2,j}); \quad u_{2,j} = c\int a(t)\cos\left(\omega_{A_{2,j}} t\right)dt \tag{14}$$

where $v_{1(2),i(j)}$ and $u_{1(2),i(j)}$ are the state and linear activation, respectively, of the $i^{th}(j^{th})$ recalled bits for i=0,1,….N_1-1 (j=0,1,….N_2-1), c is the learning rate which should be sufficiently small compared to any natural saturation limits that might be forced on u, and $\omega_{A1,i}$ and $\omega_{A2,j}$ are the 1st and 2nd virtual layer *analysis frequencies*, respectively, which are indexed from highest to lowest,

$$\omega_{A_{1,i}} := \omega_{A1.H} - N_2 i\Delta\omega\,, \qquad \omega_{A_{2,j}} := \omega_{A2.H} - j\Delta\omega \tag{15}$$

where $\omega_{A1.H}$ and $\omega_{A2.H}$ are the highest frequencies in the respective band. Initial activations should be set to small values on one side or the other of the quantizer, since the more deeply the quantizers are driven into saturation, the longer it takes to pull them back out, if necessary. The sign of initial activations may be determined by the state of the decoder in the previous decoding period.

Anti-Aliasing Constraints

Not all frequencies facilitate error-free encoding and recall. To avoid aliasing in memory formation, $\omega_{S1.L}$ must be greater than half the bandwidth of the 2nd encoding wave. This is the *encoding constraint*, which is the tightest constraint on $\omega_{S1.L}$ only when the upper side-band of the attractor wave is filtered out before transmission. Otherwise $\omega_{S1.L}$ is bound by the 2nd decoding constraint given below.

To avoid side-band aliasing of the neural activation wave, the lowest attractor frequency, $\omega_{W.LSB.L}$, must satisfy the *1st decoding constraint,*

$$\omega_{W.LSB.L} > \frac{B_{V1} + B_{V.GAP}}{2}; \qquad B_{V1} = N_2(N_1 - 1)\Delta\omega \tag{16}$$

where B_{V1} is the bandwidth of the 1st virtual layer state wave and $B_{V.GAP}$ is the gap between the 1st and 2nd virtual layer state waves, which must be greater than max(B_{V1},B_{V2}) to avoid interlayer aliasing, where B_{V2} is the bandwidth of the 2nd virtual layer state wave.

If the upper side-band of the attractor wave is not filtered out before transmission, it must be high enough not to alias the lower side-band of the *activation* wave in the decoder. This places a lower bound on $\omega_{S1.L}$, the *2nd decoding constraint*, which is more restrictive than the encoding constraint,

$$\omega_{W.USB.L} - \omega_{V2.H} > \omega_{V2.L} - \omega_{W.LSB.L}; \qquad \omega_{W.USB.L} = \omega_{S1.L} + \omega_{S2.L} \tag{17}$$

where $\omega_{W.USB.L}$ is the lowest upper side-band frequency, $\omega_{V2.L}$ and $\omega_{V2.H}$ are the lowest and highest frequencies of the 2nd virtual layer state wave. From these constraints, arbitrary frequency sets may be derived in terms of N_1 and N_2. One such set is given in (18)-(23) where the encoder frequencies are given by,

$$\omega_{S_{1,i}} := \left(\frac{7}{2}N_1N_2 - 2N_2 + \frac{1}{2} - iN_2\right)\Delta\omega + B'', \quad B'' > 0 \tag{18}$$

[2] *Even* synchronization means that oscillations are *simultaneously peaked* (cosine waves). Sine waves, on the other hand, are *oddly* synchronized; i.e. *simultaneously null*.

$$w_{S_{2,i}} = \left(\frac{9}{2}N_1N_2 - 3N_2 + \frac{3}{2} + i\right)\Delta w + B'' \quad (19)$$

for i=0,1,…., N_1-1 and j=0,1,….N_2-1, and virtual layer state wave frequencies are given by,

$$w_{V_{1,i}} = (2N_1N_2 - N_2 + 1 + N_2 i)\Delta w \quad (20)$$

$$w_{V_{2,j}} = (4N_1N_2 - 3N_2 + 2 + j)\Delta w \quad (21)$$

for i=0,1,…., N_1-1 and j=0,1,….N_2-1. Finally, the neural activation wave frequencies are given by,

$$w_{A_{1,i}} = (3N_1N_2 - 2N_2 + 1 - N_2 i)\Delta w \quad (22)$$

$$w_{A_{2,j}} = (N_1N_2 - j)\Delta w \quad (23)$$

for i=0,1,…., N_1-1 and j=0,1,….N_2-1.

Example

For a 5-bit heteroassociative spectral memory, where N_1=2 and N_2=3, the highest frequency in $s_1(t)$ according to (18) where $B''=1/2\Delta w$, is $w_{S1.H}=16\Delta w$.. Thus, $b_{1,0}$ is the amplitude (phase) at $16\Delta w$ and $b_{1,1}$ is at $(16\text{-}3)\Delta w = 13\Delta w$. According to (19), $b_{2,0}$ is the amplitude (phase) at $20\Delta w$, $b_{2,1}$ is at $21\Delta w$, and $b_{2,2}$ is at $22\Delta w$. After spectral convolution in the encoder, the attractor frequencies fall at $4\Delta w$, $5\Delta w$, etc. According to (20), the 1st frequency in the 1st virtual layer state wave, which corresponds to the 1st recalled bit in the 1st virtual layer, is placed at $10\Delta w$. The frequencies in the 2nd virtual layer state wave must be placed at $17\Delta w$, $18\Delta w$, and $19\Delta w$, according to (21). After spectral convolution in the decoder, neural activations for 1st layer neurons fall at $13\Delta w$ and $10\Delta w$, respectively, and those for 2nd layer fall at $6\Delta w$, $5\Delta w$, and $4\Delta w$, respectively, according to (22) and (23).

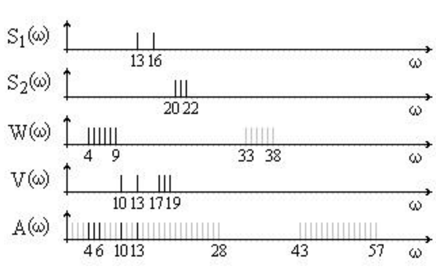

Fig. 3. Spectrums of a 5-bit (2,3 partitioned) heteroassociative spectral memory.

SINGLE-ATTRACTOR NETWORKS FOR DIGITAL COMMUNICATIONS

Spectral associative memories with single attractors lend themselves to digital communications. Binary data vectors may be transmitted as *transient spectral attractors*, one at a time, over a noisy channel to a spectral decoder. When only one attractor activates the decoder at a time, the initial conditions have no bearing on the steady state and the encoded bit vector may be recovered with exceptional noise immunity. Very low bit error rates (BER) may be achieved with relatively few neurons. Heteroassociative memories offer a compromise between redundancy and bandwidth.

Noise Immunity

Spectral associative memories must tolerate *two* sources of noise: 1) initial condition noise and 2) attractor noise. In the conventional formulation, attractor noise is not significant and is typically ignored, but it is primarily *this* noise that spectral memories must tolerate. In general, the received attractor wave, $r(t)$, may be a noisy version of the transmitted attractor wave $w(t)$. See Figure 4. Assuming an additive noise model, $r(t)$ is given by,

$$r(t) = w(t) + n(t) \quad (24)$$

where $n(t)$ is typically modeled as additive white Gaussian noise. Four main factors influence noise immunity: 1) convergence time, 2) code rate, 3) degree of spectrum spread, and 4) initial conditions. These are treated individually below.

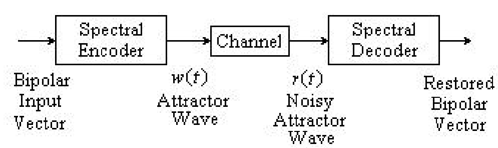

Fig. 4. Transmission of spectral attractors over a noisy channel.

Convergence Time. BER always decreases with increasing convergence time, T_c, in the presence of white noise. Fortunately, white noise cannot move the state of the system *anywhere over time* because it provides no *colored motive*. Only the *systematic* part of the attractor wave instantiates the energy landscape over time. However, T_c must be limited as $1/T_c$ is the data rate.

Code Rate. Heteroassociative code rates are determined by codeword partitioning. Attractor waves consist of N_1N_2 frequencies, where $N_1+N_2=N$. The code rate of bits in the shortest virtual layer are always the higher than those in the longest layer and these bits are encoded with the most redundancy and highest noise immunity. The symbol-to-bit ratio of 1st layer bits is N_2:1 and the symbol-to-bit ratio of

2^{nd} layer bits is N_1:1. Therefore, most significant bits may be placed in the shortest virtual neural layer.

Spectrum Spread. The degree to which information is "spread out" over the frequency domain also influences noise immunity and is somewhat related to the popular concept of *spread spectrum*. Spectrum spread is directly controled by the radial frequency separation parameter, Δw, which increaces the level of tolerable noise. Specifically, the bandwidth of the lower side-band of the attractor wave is given by,

$$B_{W.LSB.L} = B_{S1} + B_{S2} = (N_1 N_2 - 1)\Delta w \qquad (25)$$

where B_{S1} and B_{S2} are the bandwidths of the 1^{st} and 2^{nd} encoding waves, respectively.

Initial Conditions. In general, initial conditions may be fixed, from decoding period to decoding period, but if successive codewords are samples of a continuous quantity, linear activations may be initialized according to the previous state. As long as the initial values are not too large, BER may be reduced by carrying over state information.

BER is shown in Figure 5 for a 5-bit heteroassociative code, partitioned into two virtual layers with N_1=2 and N_2=3, for increasing SNR and various degrees of spectrum spread and convergence time with fixed initial conditions where linear SNR was observed to be,

$$SNR_{linear} = \frac{\frac{1}{K}\sum_{k=0}^{K-1} w^2(kT)}{\frac{1}{K}\sum_{k=0}^{K-1} n^2(kT)} = \frac{P_s}{s^2}; \quad T_c = KT \qquad (26)$$

where K was the integer number of iterations per decoding period, s^2 was the noise power, T was the sample period, and T_c was the convergence time. The decoder effectively bandlimited the noise at the same rate as the signal, $1/T_c$, thus the power ratio was the same as the energy ratio.

One bit of overhead in the 1^{st} virtual layer was used to distinguish between complementary attractor states. Since N_2>N_1, the 1^{st} layer bits are more immune to noise than 2^{nd} layer bits and the reference bit is by far the most significant. The decoder was perfectly synchronized with the encoder, all blocks were assumed to be ideal, and the upper side-band of the attractor wave was not filtered out.

At this time, it appears that both autoassociative and heteroassociative SAMs outperform turbo decoders for equal block lengths, due to the high encoding redundancy of spectral associative memories. When compared in terms of equal code rate, 5-bit SAMs appear to outperform turbo decoders with block lengths of over 1024 bits in high noise conditions (<0dB SNR), but further studies are needed to say for sure.

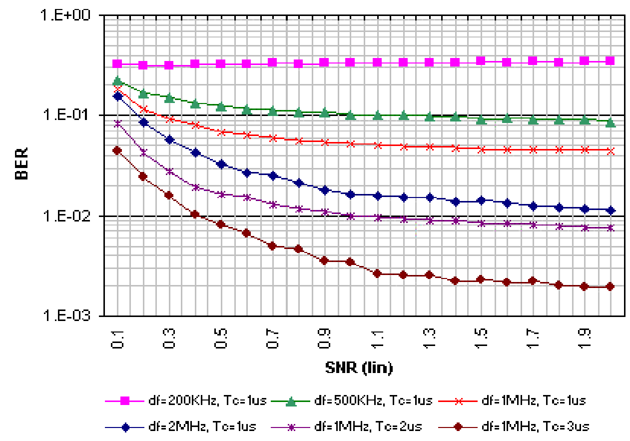

Fig. 5. Bit error rates for a 5-bit heteroassociative spectral code partitioned into two virtual layers of N_1=2 and N_2=3 for increasing SNR and various degrees of spectrum spread and convergence time. (1μs = 1000 iterations, $\Delta\omega = 2\pi\Delta f$)

IMPLEMENTATION AND SCALING COMPLEXITY

Linear scalability is realized while maintaining the high symbol-to-bit ratios of the spatial formulations. By contrast, the non-spectral formulation of the bidirectional associative memory scales polynomially.

Non-Multiplexed Decoding

The heteroassociative spectral encoder for N-bit codewords requires N oscillators (O), two summers (S), and one mixer (M),

$$Encoder(N) = NO + 2S + M \qquad (27)$$

which represents a savings of N oscillators over the autoassociative encoder. The general non-multiplexed spectral decoder requires 2N oscillators, one summer, N+1 mixers, N integrators (I), and N bipolar comparators (C),

$$Decoder_{Non-mult.}(N) = M + S + N(2O + M + I + C). \qquad (28)$$

Notice that both encoder and decoder scale independently of codeword partitioning. Only the frequencies determine virtual partitioning.

Multiplexed Decoding

The spectral decoder may be multiplexed, further reducing the complexity. Each neuron should be updated asynchronously anyway to avoid limit cycles. Such a decoder would require N+1 oscillators, one summer, two mixers, one integrator, and N memory elements (Q),

$$Decoder_{Mult.Digital}(N) = O + S + 2M + I + N(O+Q) \qquad (29)$$

In mixed-mode circuit implementations, summation is often performed in the current domain. In such implementations, capacitors (*CAP*) may act simultaneously as integrators and memory elements, and inverters (*T*) may be used to quantize the activations, as shown in Figure 6,

$$Decoder_{Mult.Analog}(N) = O + 2M + N(O + CAP + T) \qquad (30)$$

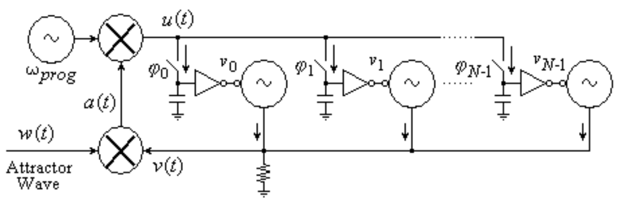

Fig. 6. Schematic of one possible current-mode multiplexed spectral decoder.

CONCLUSIONS

Heteroassociative spectral memories were introduced as an extension of autoassociative spectral memories, recurrent associative memories realized in the frequency domain in which the attractors are represented as a superposition of waves. Rather than being embedded in the neural decoder, spectral attractors exist separately from the decoder and can be used to transmit digital information over a noisy channel. Linear scalability is achieved by realizing non-local connectivity in the frequency domain, without compromising high symbol-to-bit ratios, which provide noise immunity. BERs of less than 10^-4 may be achieved with autoassociative spectral encoders and decoders for signals no stronger than the noise itself, making autoassociative SAMs strong candidates for robust digital telecommunications. Yet, the encoding redundancy of the autoassociative memory is forced to be N:1, which causes the bandwidth of the attractor wave to scale quadratically with bit vector dimension. Heteroassociative spectral memories offer a compromise between encoding redundancy and bandwidth for the same number of bits. In the same way that bidirectional associative memories reduce the encoding redundancy and scaling complexity of N-dimensional spatial Hopfield networks partitioned into two neural layers, heteroassociative spectral memories reduce the bandwidth of the attractor wave of autoassociative spectral memories. Furthermore, heteroassociative encoders require half the number of oscillators as autoassociative encoders, making an already simple architecture, simpler. Simulations were presented that show BER vs. SNR for various degrees of spectrum spread and convergence time for a heteroassociative partitioning of 5-bit codewords in the presence of white noise.

REFERENCES

Chua, L., Roska, T., and Venetianer, P., 1993, "The CNN is as Universal as the Turing Machine", *IEEE Trans. on Circuits and Systems*, Vol. 40, No.4, pp.289-291.

Gabor, D., 1969, "Associative holographic memories," *IBM J. Res. Dev.*, Vol. 156.

Hopfield, J., 1982, "Neural networks and physical systems with emergent collective computational abilities," *Proc. National Academy of Sciences*, Vol. 79, pp. 2554-2558.

Jibu M. and Yasue, K., 1993, "The basics of brain dynamics," in *Rethinking Neural Networks: Quantum Fields and Biological Data*, K. Pribram (Ed.), Lawrence Erlbaum Assoc., pp. 121-145.

Jibu M. and Yasue, K., 1995, *Quantum brain dynamics and consciousness*, John Benjamins Publishing Co.

Kosko, B., 1987, "Adaptive bidirectional associative memories," *Applied Optics*, Vol. 26, No. 23, pp. 4947-4959.

Kosko, B., 1988, "Bidirectional associative memories," *IEEE Trans. On Systems, Man, and Cybernetics*, Vol. 18, No. 1, pp. 49-60.

Owechko, Y., 1989, "Nonlinear holographic associative memories," *IEEE J. of Quantum Elect.*, vol. 25, no. 3.

Psaltis, D. and Farhat, N., 1985, "Optical information processing based on an associative-memory model of neural nets with thresholding and feedback," *Optics Letters*, Vol. 10, p. 98.

Psaltis, D., Brady, D., Gu, X., and Lin, S., 1990, "Holography in artificial neural networks," *Nature*, Vol. 343, pp. 325-330.

Schrödinger, E., 1926, "Qiantisierung als Eigenwertproblem," (I, II and III), *Annalen der Physik*, Vol. 79, pp. 361-376 and 489-527, and Vol. 80, pp. 437-490.

Spencer, R., 2000, "Nonlinear spectral associative memories: Neural encoders and decoders for digital communications," to appear at *ANNIE 2000*, St. Louis, Missouri, Nov. 5-8, 2000.

Ventura, D. and Martinez, T., 1998, "Quantum associative memory with exponential capacity," *IEEE Int'l. Joint Conference on Neural Networks*, Vol. 1, pp. 509-513.